Dynamics of positrons during relativistic electron runaway

O. Embréus[1], K. Richards[1], G. Papp[2], L. Hesslow[1], M. Hoppe[1], T. Fülöp[1]

[1]*Chalmers University of Technology, SE-41295, Göteborg, Sweden*

[2]*Max-Planck-Institute for Plasma Physics, D-85748 Garching, Germany*

Positrons are ubiquitous in systems involving particles with kinetic energy exceeding the pair-production threshold energy $2m_ec^2 \approx 1\,\mathrm{MeV}$. Relativistic electron runaway constitutes a class of such systems, whereby an electric field strong enough to overcome the dynamical collisional friction for suprathermal test particles can accelerate a significant population of electrons to average energies in the 10 MeV range [1, 2]. Runaway breakdown is believed to be an important mechanism of lightning initiation, and is also actively researched in the context of nuclear-fusion energy production due to the detrimental effect on the first wall of runaway electrons created during tokamak disruption events.

The general characteristics of the positron dynamics during runaway is as follows. Runaway electrons are accelerated in the direction opposite to the electric field, typically having small characteristic pitch angles. The energy spectrum tends to be exponentially decaying with an average energy $\gamma_0 m_e c^2$ of tens of MeV, and the total number of runaway electrons increases exponentially in time due to the avalanche mechanism [2]. The runaway electrons produce electron-positron pairs, which typically have highly relativistic velocities aligned with the incident electron. The positrons generated during runaway – having the opposite charge of electrons – are thus initially moving opposite to their direction of acceleration in the electric field, and only a fraction of positrons will become runaway accelerated themselves; the remainder become thermalized and promptly annihilate.

The runaway dynamics described above can be most clearly captured in a homogeneous plasma, in which case it is governed by the positron kinetic equation

$$\frac{\partial f_{\mathrm{pos}}}{\partial t} + eE\left[\xi\frac{\partial}{\partial p} + \frac{1-\xi^2}{p}\frac{\partial}{\partial \xi}\right] f_{\mathrm{pos}} = C_{\mathrm{pos}} + S_{\mathrm{pos}} + S_{\mathrm{an}}, \tag{1}$$

where f_{pos} is the positron distribution function at time t and momentum $\mathbf{p} = \gamma m_e \mathbf{v}$, where the positron velocity is denoted $\mathbf{v}$ and $\gamma = 1/\sqrt{1-v^2/c^2}$, $\xi \equiv \cos\theta = \mathbf{p}\cdot\mathbf{E}/pE$ is the pitch-angle cosine, C_{pos} is the positron collision operator, S_{pos} denotes the source term of positrons generated in collisions between relativistic runaway electrons and field particles of the plasma, as well as positron production by highly energetic photons, and S_{an} denotes the annihilation term. Since the positron-electron scattering cross section equals the electron-electron cross section to leading order in the small scattering angle, the positron collision operator C_{pos} equals the

electron collision operator to leading order in the Coulomb logarithm $\ln\Lambda$. Thus, the positron Fokker-Planck equation differs from the corresponding electron equation only through the opposite direction of acceleration in the electric field, as well as the presence of creation and annihilation terms. The source term is given by

$$S_{\rm pos} \equiv \left(\frac{\partial f_{\rm pos}}{\partial t}\right)_{\rm pp} = \sum_i n_i c \left[\int {\rm d}\mathbf{p}_1 \, \frac{v_1}{c} \frac{\partial \sigma^+_{ci}}{\partial \mathbf{p}} f_{\rm RE}(\mathbf{p}_1) + \int {\rm d}\mathbf{k} \, \frac{\partial \sigma^+_{\gamma i}}{\partial \mathbf{p}} \phi_\gamma(\mathbf{k}) \right], \tag{2}$$

summed over all species i in the plasma. In the first term, $f_{\rm RE}$ is the runaway-electron distribution and σ^+_{ci} is the cross-section for the creation of a positron in an electron-ion collision evaluated using MadGraph 5 [3]. In the second term, ϕ_γ is the photon distribution and $\sigma^+_{\gamma i}$ is the Bethe-Heitler cross-section for pair production by a photon in the field of a nucleus [**?**]. Since the scattering time of highly energetic photons tends to be significantly longer than the avalanche time $t_{\rm ava} = f_{\rm RE}/(\partial f_{\rm RE}/\partial t)$, the photon distribution in a homogeneous plasma is given by $\phi_\gamma = t_{\rm ava} \sum_i n_i \int {\rm d}\mathbf{p}_1 \, v_1 (\partial \sigma_{{\rm br},i}/\partial \mathbf{k}) f_{\rm RE}(\mathbf{p}_1)$ where $\sigma_{\rm br}$ is the bremsstrahlung cross section for the emission of a photon with momentum $\mathbf{k}$ by an incident electron with momentum $\mathbf{p}_1$. At the ultra-relativistic energies that we consider, the bremsstrahlung cross section ${\rm d}\sigma_{\rm br}$ and pair-production cross sections ${\rm d}\sigma_c$ and ${\rm d}\sigma_\gamma$ are all sharply peaked around the direction of the incident electron. Then, by neglecting the angle between incident runaway electron and created positron, the source term takes the form

$$S_{\rm pos}(p, \cos\theta) = \frac{n_e Z_{\rm eff} m_e c^2}{p\gamma} \int_{\gamma+2}^\infty {\rm d}\gamma_1 \, p_1^2 \frac{\partial \sigma^+}{\partial \gamma} f_{\rm RE}(\gamma_1, \cos\theta), \tag{3}$$

$$\frac{\partial \sigma^+}{\partial \gamma} = \frac{\partial \sigma^+_c}{\partial \gamma}(\gamma, \gamma_1) + \frac{(Z_{\rm eff}+1)^2}{Z_{\rm eff}} t_{\rm ava} n_e c \int_{\gamma+1}^{\gamma_1 - 1} {\rm d}k \, \frac{\partial \sigma^+_\gamma}{\partial \gamma}(\gamma, k) \frac{\partial \sigma_{\rm br}}{\partial k}(k, \gamma_1). \tag{4}$$

Since all the cross sections σ_{xi} used here scales with ion charge as Z_i^2, we have written for short $\sum_i n_i \sigma_{xi} = n_e Z_{\rm eff} \sigma_x$. The avalanche time is given by $t_{\rm ava} = c_Z/[4\pi n_e r_0^2 c(E/E_c - 1)]$ with $r_0 = e^2/(4\pi\varepsilon_0 m_e c^2)$ and c_Z an order-unity parameter which is insensitive to electric field, calculated in Ref. [**?**] to be $c_Z \approx \sqrt{5 + Z_{\rm eff}}$. The energy spectrum of avalanching runaway electrons is given by $p^2 \int f_{\rm RE}(\mathbf{p}, t) {\rm d}\Omega \approx e^{t/t_{\rm ava} - \gamma/\gamma_0}$ where $\gamma_0 = c_Z \ln\Lambda$. From this expression it follows that there exists a threshold electric field $E_{\rm pp}$ above which pair production in collisions is more important than that via bremsstrahlung photons, which is given by

$$\frac{E_{\rm pp}}{E_c} - 1 = \frac{(1+Z_{\rm eff})^2}{Z_{\rm eff}} \frac{c_Z}{4\pi r_0^2} \frac{\int_3^\infty {\rm d}\gamma_1 \, e^{-\gamma_1/\gamma_0} \int_2^{\gamma_1 - 1} {\rm d}k \, \sigma^+_\gamma(k) \frac{\partial \sigma_{\rm br}}{\partial k}(k, \gamma_1)}{\int_3^\infty {\rm d}\gamma_1 \, e^{-\gamma_1/\gamma_0} \sigma^+_c(\gamma_1)} \approx 3.25 c_Z \frac{(1+Z_{\rm eff})^2}{Z_{\rm eff}}, \tag{5}$$

where the last approximation has an error of less than a few percent for $20 < \gamma_0 < 80$, and $E_c = n_e \ln\Lambda e^3/4\pi\varepsilon_0^2 m_e c^2$ is the avalanche threshold field. Thus, $E_{\rm pp} \approx 30$ for $Z_{\rm eff} = 1$, and increases with effective charge. When the linear dimension of the system is smaller than a

pair production mean free path $L_{\rm pp} \approx (3\times10^7\,{\rm m}/n_e[10^{20}\,{\rm m}^{-3}])Z_{\rm tot}/(1+Z_{\rm tot})^2$, however, pair production in collisions will always be the dominant source of positrons. In the following we shall focus on positron generation in tokamaks, for which $L \ll L_{\rm pp}$ is extremely well satisfied, with $n_e \gtrsim 10^{19}\,{\rm m}^{-3}$ and $L \sim 1\,{\rm m}$.

The positron kinetic equation admits analytic steady-state solutions in the high-energy limit and when $(1-|\xi|)\gamma E/E_c \gg Z_{\rm eff}$ is satisfied, i.e. for sufficiently small $Z_{\rm eff}$ or large E/E_c such that the energetic particles move primarily (anti-)parallel to the electric field. Annihilation can generally be neglected, since the annihilation cross section is only significant for thermalized positrons. By introducing an extended momentum coordinate p and the half-plane averaged positron distribution

$$\mathscr{F}(p,t) = 2\pi p^2 \times \begin{cases} \int_{-1}^{0} {\rm d}\xi\, f(|p|,\xi), & p<0 \\ \int_{0}^{1} {\rm d}\xi\, f(p,\xi), & p\geq 0 \end{cases} \tag{6}$$

the kinetic equation takes the form

$$\frac{\partial \mathscr{F}(p,t)}{\partial t} + eE_c\left(\frac{E}{E_c}-{\rm sgn}(p)\right)\frac{\partial \mathscr{F}(p,t)}{\partial p} = n_e c Z_{\rm eff}\int_{\gamma+2}^{\infty}{\rm d}\gamma_1\,\frac{\partial\sigma^+}{\partial\gamma}(\gamma,\gamma_1)\mathscr{F}_{\rm RE}(p_1,t), \tag{7}$$

where $p_1 = {\rm sgn}(p)\sqrt{\gamma_1^2-1}$ and $\mathscr{F}_{\rm RE}=0$ for $p_1>0$ and $\mathscr{F}_{\rm RE} = (m_e c\gamma_0)^{-1} n_{\rm RE}\exp(-\gamma_1/\gamma_0)$ for $p_1<0$, and $n_{\rm RE} = n_0 e^{t/t_{\rm ava}}$. The equation admits an analytic solution for the positron distribution, which is given by

$$\mathscr{F} = \begin{cases} \frac{Z_{\rm eff}}{4\pi\ln\Lambda r_0^2}\frac{n_{\rm RE}}{\gamma_0 m_e c}\int_{\gamma}^{\infty}{\rm d}\gamma'\int_{\gamma'+2}^{\infty}{\rm d}\gamma_1\,\frac{\partial\sigma^+}{\partial\gamma'}(\gamma',\gamma_1)\exp\left[-\frac{\gamma_1+\rho(\gamma'-\gamma)}{\gamma_0}\right], & p<0 \\ \frac{n_{\rm RP}}{m_e c\gamma_0}e^{-\gamma/\gamma_0}, & p>0 \end{cases} \tag{8}$$

where $\rho = (E/E_c-1)/(E/E_c+1)$, and where the runaway positron density is $\int_0^\infty {\rm d}p\,\mathscr{F} \approx n_{\rm RP}(t) = n_{\rm RP}(0)e^{t/t_{\rm ava}}$. In Fig. 1 we show the analytic solutions for two different cases, as well as numerically obtained quasi steady state solutions using the kinetic solver CODE [4], to which the positron creation and annihilation terms have been added. Excellent agreement is found between the solutions, particularly when $E/Z_{\rm eff}$ is large, as predicted.

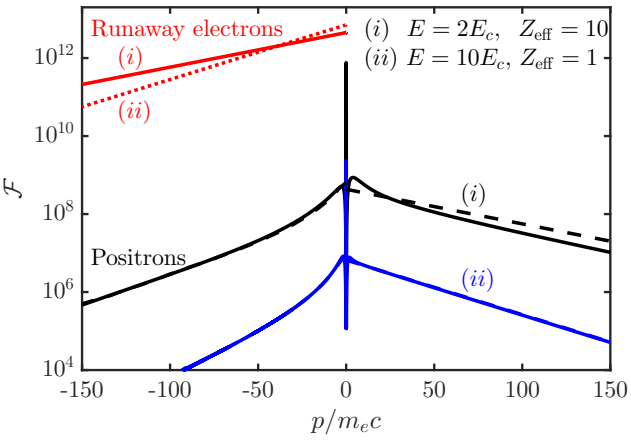

Figure 1: Runaway electron and positron distributions illustrated by solid (numerical solutions) and dashed (analytical) lines for two different scenarios.

By numerically solving for the quasi steady state positron distribution, we have determined the steady state ratio $n_{\mathrm{RP}}/n_{\mathrm{RE}}$ as a function of background electric field and plasma charge, which is found to be maximized when $E \approx 2E_c$, at which point it approximately takes the value $n_{\mathrm{RP}}/n_{\mathrm{RE}} \approx 8.5 \cdot 10^{-7} Z_{\mathrm{eff}} c_Z (c_Z - 0.45)$; this is small enough that it is unlikely that the positron-emitted synchrotron and HXR radiation will be be distinguishable from the background electron emission. However, since a fraction of the created positrons thermalize and promptly annihilate, their annihilation radiation – which is sharply peaked around 511 keV – may be visible through the continuous X-ray background of runaways. We characterize the signal-to-noise ratio of the annihilation radiation to the continuous HXR spectrum of the runaway electrons by

$$\Delta k = \frac{\partial n_{\mathrm{an}}/\partial t \partial \Omega}{\partial n_{\mathrm{HXR}}/\partial t \partial \Omega \partial k} = \eta \frac{\int_3^\infty \mathrm{d}\gamma_1 \, \sigma^+(\gamma_1) \mathscr{F}_{\mathrm{RE}}/4\pi}{\int_{\gamma > k+1} \mathrm{d}\mathbf{p} \, v \frac{\partial \sigma_{\mathrm{br}}}{\partial k \partial \Omega} f_{\mathrm{RE}}(\mathbf{p})}, \tag{9}$$

i.e. the ratio of the annihilation photon flux to the spectral HXR photon flux, where η is the fraction of created positrons that slows down, which depends sensitively on E and Z_{eff}. Δk can be interpreted as the energy resolution of a detector required for the annihilation peak to protrude with twice the amplitude of the continuous HXR background. This will be maximized for detection at an angle perpendicular to the direction of acceleration; evaluation of Δk with numerical solutions for the runaway distribution and thermalization fraction η is shown in Fig. 2, and we observe an approximate scaling $\Delta k \approx 7\,\mathrm{keV}/\sqrt{1+Z_{\mathrm{eff}}}$.

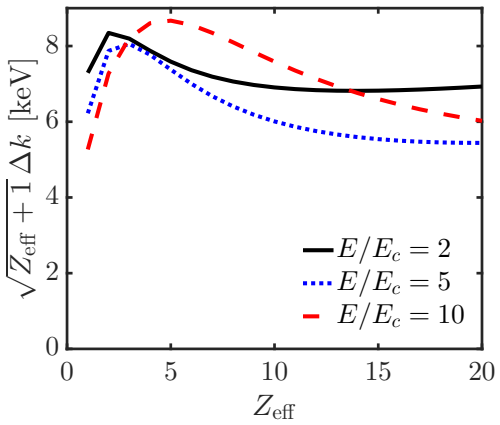

Figure 2: Resolution parameter Δk for detection of the positron annihilation peak during electron runaway.

With a detector photon-energy resolution finer than this, the annihilation peak due to thermalized positrons created during electron runaway is predicted to be well distinguishable from the HXR. If the energy resolution is below Δk, coincidence measurements can be employed to improve signal-to-noise, although this requires a relatively stronger signal.

References

[1] A. V. Gurevich *et al.*, Phys. Lett. A **165**, 463 (1992)

[2] M. N. Rosenbluth *et al.*, Nucl. Fusion **37**, 1355 (1997)

[3] J. Alwall *et al.*, J. High Energy Phys. **7**, 79 (2014)

[4] M. Landreman et al., Comp. Phys. Comm. **185**, 847 (2014).